Ship Dynamic Positioning Output Feedback Control with Thruster System Dynamics

Dongdong Mu*
College of Marine Electrical Engineering
Dalian Maritime University
Dalian, China
ddmu@dlmu.edu.cn

Xiaomeng He
College of Marine Electrical Engineering
Dalian Maritime University
Dalian, China
892374020@qq.com

Qiulin Lu
Qinhuangdao Ecological Environment Monitoring Center of Hebei Province
Qingdao, China
13833582885@ 139.com

Yunsheng Fan
College of Marine Electrical Engineering
Dalian Maritime University
Dalian, China
yunsheng@dlmu.edu.cn

Fei Pang
College of Marine Electrical Engineering
Dalian Maritime University
Dalian, China
pangfei @dlmu.edu.cn

Fei Wang
College of Marine Electrical Heating company
Dalian Clean Energy Group
Dalian, China
1285909356@ qq.com

Beibei Li
College of Marine Electrical Engineering
Dalian Maritime University
Dalian, China
2529606589@qq.com

Mingyang Yin
College of Marine Electrical Engineering
Dalian Maritime University
Dalian, China
18340687776@163.com

2024 9th International Conference on Automation, Control and Robotics Engineering (CACRE) | 979-8-3503-5030-2/24/$31.00 ©2024 IEEE | DOI: 10.1109/CACRE62362.2024.10635087

***Abstract*—In this paper, a novel backstepping controller considering thruster system dynamics is proposed. Firstly, a practical ship dynamic positioning control algorithm is formulated leveraging the thruster system dynamics, along with a finite-time convergent disturbance observer and an auxiliary dynamic system designed for finite-time convergence. The designed dynamic positioning closed-loop control system is uniformly ultimately stable. The advantages of the developed control scheme are that first, it addresses a multitude of potential challenges that the dynamic positioning system could encounter amidst intricate sea conditions, which is conducive to the implementation of the algorithm in maritime practice; Second, thruster system dynamics were considered to ensure smooth changes in actual control variables, aligning more closely with engineering realities. Finally, the control's effectiveness stays consistent. algorithm was validated through simulation, reinforcing its practical applicability.**

Keywords— Dynamic Positioning; Unmeasurable Speed; External Disturbances;

I. INTRODUCTION

Ship dynamic positioning technology is a kind of positioning technology applied to the ship to keep floating automatically at sea without mooring. With the development and progress of marine technology, ship dynamic positioning has also been gradually developed. The initial dynamic positioning system relies on a linear control approach. which is ineffective due to the highly nonlinear ship model. As nonlinear control technology advances, the control strategy for ship dynamic positioning systems progressively transitions from linear to nonlinear methods.

In practice, accurately gathering both position and velocity data can be challenging. Additionally, classification society standards mandate that when a ship's sensors fail, observers must supply the necessary information. The integration of a state observer into the dynamic positioning control system enables dynamic positioning control to be achieved effectively by solely utilizing the vessel's location and directional data [1]. Hence, the dynamic positioning system's output feedback controller, which employs an observer, demonstrates remarkable fault tolerance [2].

The thruster's capacity to generate adequate thrust, following the directives of the control algorithm, remains a pivotal aspect of the ship's dynamic positioning system [3]. The thruster, capable of generating the required thrust to maintain the ship in the desired position and heading according to the control algorithm, is an important component of the ship's dynamic positioning system [4].

When operating within a genuine marine context, the operational limitations of the thrusters and external environmental interferences on their blades hinder them from fully executing the control signal and generating the intended thrust, ultimately leading to a reduction in thrust efficiency [5]. Consequently, for practical applications, it becomes imperative to incorporate the thruster system dynamics equation into the control law design process. This ensures that the generated

This work was supported by National Key Research and Development Program of China(Grant number 2022YFB4301401), National Natural Science Foundation of China (Grant number 52301360), Pilot Base Construction and Pilot Verification Plan Program of Liaoning Province of China (Grant number 2022JH24/10200029), Fundamental Research Funds for the Central Universities (Grant number 3132024101), China Postdoctoral Science Foundation (Grant number 2022M710569), Liaoning Province Doctor Startup Fund (Grant number 2022-BS-094) and Dalian Key Science and Technology Research and Development Plan (Grant number 2023YF11GX007).

control signal enables the actual thrust outputted by the thruster to achieve an optimal control effect.

Building upon the aforementioned considerations, this paper also takes into account unmeasurable ship speed, external disturbances, and input saturation. and thruster system dynamic simultaneously for the first time in a dynamic positioning output feedback control system [6]. This paper's primary contributions can be summarized as follows:

1) To enhance its practical relevance, this paper considers an extensive range of potential challenges that the dynamic positioning system may encounter in intricate marine environments.

2) The utilization of a finite-time convergence disturbance observer effectively addresses unknown disturbances, resulting in a substantial improvement in convergence rate when compared to a conventional disturbance observer.

II. Problem Formulation and Preliminaries

A. Problem formulation

Dynamic positioning mathematical model with thruster system dynamic can be described as

$$\dot{\eta} = J(\psi)v \tag{1}$$

$$M\dot{v} = -Dv + \tau + \tau_d \tag{2}$$

$$\dot{\tau} = -A_{tr}\tau + A_{tr}\tau_p \tag{3}$$

where $\eta = [x, y, \psi]^{\mathrm{T}}$ indicates the position of the ship in the north-east coordinate system, where x, y, and ψ are used as the surge position, sway position and heading respectively. $J(\psi) \in R^{3\times3}$ indicates the following rotation matrix given by

$$J(\psi) = \begin{bmatrix} \cos(\psi) & -\sin(\psi) & 0 \\ \sin(\psi) & \cos(\psi) & 0 \\ 0 & 0 & 1 \end{bmatrix} \tag{4}$$

where $\mathrm{J}^{-1}(\psi) = \mathrm{J}^{\mathrm{T}}(\psi)$ and $\| \mathrm{J}(\psi) \| = 1$. $\mathrm{M} \in \mathrm{R}^{3\times3}$ is an inertia matrix. $D \in R^{3\times3}$ is a hydrodynamic damping matrix. $\tau = [\tau_1, \tau_2, \tau_3]^{\mathrm{T}}$

$$\tau_{pi} = \mathrm{sat}(\tau_{ci}) = \begin{cases} \mathrm{sgn}(\tau_{ci})\tau_{Mi} & |\tau_{ci}| \geq \tau_{Mi} \\ \tau_{ci} & |\tau_{ci}| < \tau_{Mi} \end{cases}, i = 1,2,3 \tag{5}$$

where $\tau_{Mi} > 0$ indicates the saturation limits, $\tau_c = [\tau_{c1}, \tau_{c2}, \tau_{c3}]^{\mathrm{T}}$ indicates the commanded thrust force and moment vector. The difference between τ_p and τ_p is $\Delta\tau = \tau_p - \tau_c$.

III. Design of Ship Dynamic Positioning Control System

A. Design of high-gain state observer

In practice, $\eta(t)$ and its first derivative $\dot{\eta}(t)$ are bounded. The high-gain state observer is constructed as follows:

$$\begin{cases} \delta\dot{\pi}_1 = \pi_2 \\ \delta\dot{\pi}_2 = -\lambda_1\pi_2 - \pi_1 + \eta(t) \end{cases} \tag{6}$$

where $\pi_1, \pi_2 \in R^3$ are the state vectors of the high-gain observer. The estimations of $\eta(t)$ and its first derivative $\dot{\eta}(t)$ are

$$\hat{\eta} = \pi_1 \tag{7}$$

$$\hat{\dot{\eta}} = \frac{1}{\delta}\pi_2 \tag{8}$$

Hence, according to (8) and (1), the estimation $\hat{v}$ can be shown as

$$\hat{v} = J^T(\psi)\left(\frac{1}{\delta}\pi_2\right) \tag{9}$$

According to (7), we get

$$\begin{aligned} \hat{\eta} - \eta &= \pi_1 - \eta \\ &= -\dot{\bar{\delta}}\psi \end{aligned} \tag{10}$$

According to (10), we get

$$\| \hat{\eta} - \eta \| = \delta \| \hat{\psi} \| \leq \delta B_1 \tag{11}$$

where B1 is a positive constant.

Similarly, according to (1), (9), $J^{-1}(\psi) = J^T(\psi)$

$$\hat{v} - v = -\delta J^T(\psi)\dot{\bar{\psi}} \tag{12}$$

According to (12), $\| J(\psi) \| = 1$,we get

$$\| \hat{v} - v \| = \delta \| \ddot{\bar{\psi}} \| \leq \delta B_2 \tag{13}$$

where B2 is a positive constant.

B. Design of finite-time convergent disturbance observer

In this paper, a finite-time convergent disturbance observer is used to estimate the unknown as

$$\tilde{p} = \hat{p} - p \tag{14}$$

The differential equation for constructing the estimation error $\tilde{p}$ is

$$\dot{\tilde{p}} = -D_1\tilde{p} - D_2|\tilde{p}|^\gamma sgn(\tilde{p}) - \bar{\tau}_d sgn(\tilde{p}) - \tau_d \tag{15}$$

According to (2), (8), (9), the derivation of $\hat{p}$ gives

$$\dot{\hat{p}} = -Dv + \tau - D_1\tilde{p} - D_2|\tilde{p}|^\gamma sgn(\tilde{p}) - \bar{\tau}_d sgn(\tilde{p}) \tag{16}$$

where and $D_2 = \mathrm{diag}\{D_{21}, D_{22}, D_{23}\}$ are parameter matrices, $\bar{\tau}_d$ is the disturbance upper bound vector. $0 < \gamma < 1$.

Defining $\hat{\tau}_d$ as an estimate of τ_{d}, the fixed-time convergent disturbance observer can be obtained according to (16) as

$$\hat{\tau}_d = -D_1\tilde{\mathrm{p}} - D_2|\tilde{\mathrm{p}}|^\gamma \mathrm{sgn}(\tilde{\mathrm{p}}) - \bar{\tau}_d\mathrm{sgn}(\tilde{\mathrm{p}}) \tag{17}$$

C. . Dynamics controller design

In this section, the primary focus is on designing a dynamic positioning nonlinear control scheme.

Define the error vector as follows:

$$S_1 = \eta - \eta_d \tag{18}$$

$$S_2 = v - \alpha_1 \tag{19}$$

$$S_3 = \tau - \alpha_2 \tag{20}$$

According to (1), the derivation of (18) yields

$$\dot{S}_1 = \mathrm{J}(\psi)\mathrm{v} \tag{21}$$

Select the Lyapunov function candidate as following:

$$V_1 = \frac{1}{2}S_1^T S_1 \tag{22}$$

According to (19) and (21), the derivation of (22) yields

$$\begin{aligned} \dot{\mathrm{V}}_1 &= \mathrm{S}_1^T\dot{\mathrm{S}}_1 \\ &= \mathrm{S}_1^T\mathrm{J}(\psi)(\mathrm{S}_2 + \alpha_1) \end{aligned} \tag{23}$$

Design the intermediate control function vector α1 as

$$\alpha_1 = -\mathrm{J}^T(\psi)\mathrm{K}_1 S_1 \tag{24}$$

Substituting (24) into (23), the collation gives

$$\begin{aligned} \dot{\mathrm{V}}_1 &= \mathrm{S}_1^T \mathrm{J}(\psi)\mathrm{S}_2 + \mathrm{S}_1^T \mathrm{J}(\psi)\alpha_1 \\ &= -\mathrm{S}_1^T \mathrm{K}_1 \mathrm{S}_1 + \mathrm{S}_1^T \mathrm{J}(\psi)\mathrm{S}_2 \end{aligned} \tag{25}$$

According (2), the derivative of (19) is

$$M\dot{S}_2 = -Dv + \tau + \tau_d - M\dot{\alpha}_1 \tag{26}$$

Establish the Lyapunov function candidate as following:

$$V_2 = V_1 + \frac{1}{2} S_2^T \mathrm{M} S_2 \tag{27}$$

According (25), (26), the derivative of (27) is

$$\begin{aligned} \dot{V}_2 &= \dot{V}_1 + S_2^T M \dot{S}_2 \\ &= -S_1^T K_1 S_1 + S_1^T J(\psi) S_2 + S_2^T(-Dv + \tau + \tau_d - M\dot{\alpha}_1) \end{aligned} \tag{28}$$

Define the intermediate control function vector α2 as

$$\alpha_2 = -\mathrm{K}_2 \mathrm{S}_2 - \mathrm{J}^T(\psi)\mathrm{S}_1 + \mathrm{Dv} - \hat{\tau}_d + \mathrm{M}\dot{\alpha}_1 \tag{29}$$

According to (3) and $\Delta\tau = \tau_p - \tau_c$, the derivative of (20) is

$$\begin{aligned} A_{tr}^{-1}\dot{\mathrm{S}}_3 &= A_{tr}^{-1}\dot{\tau} - A_{tr}^{-1}\dot{\alpha}_2 \\ &= -\tau + \tau_c + \Delta\tau - A_{tr}^{-1}\dot{\alpha}_2 \end{aligned} \tag{30}$$

In order to solve the input saturation, an auxiliary dynamic system is shown as follows:

$$\dot{\boldsymbol{\xi}} = \begin{cases} -K_{\xi_1}\xi - K_{\tilde{\zeta}_2}|\boldsymbol{\xi}|^{r_0} - \dfrac{\sum_{i=1}^3 |s_{3,i}\Delta\tau_i| + 0.5K_{\tilde{\zeta}_3}\Delta\tau^{\mathrm{T}}\Delta\tau}{\|\boldsymbol{\xi}\|^2} + K_{\tilde{\zeta}_3}\Delta\tau & \|\boldsymbol{\xi}\| \geq \tilde{\zeta}_0 \\ \mathbf{0}_{3\times 1} & \|\boldsymbol{\xi}\| < \tilde{\zeta}_0 \end{cases} \tag{31}$$

where $\xi = [\xi_1, \xi_2, \xi_3]^{\mathrm{T}}$ is the state vector of the auxiliary dynamic system, $\tilde{\xi}_0 > 0$ is a positive constant.

Theorem 1. The state vector $\xi = [\xi_1, \xi_2, \xi_3]^{\mathrm{T}}$ can converge to zero in finite time.

Proof of Theorem 1. Establish the Lyapunov function candidate as following:

$$V_{\mathrm{FCADS}} = \frac{1}{2}\xi^{\mathrm{T}}\xi \tag{32}$$

When $\|\boldsymbol{\xi}\| \geq \tilde{\xi}_0$, the derivative of (32) is

$$\begin{aligned} \dot{V}_{FCADS} &= \xi^T \dot{\xi} \\ &= -\xi^{\mathrm{T}} K_{\xi_1}\xi - \sum_{i=1}^{3} K_{\xi_2,i}\left|\tilde{\xi}_i\right|^{r_0+1} - \sum_{i=1}^{3}\left|s_{3,i}\Delta\tau_i\right| \\ &\quad -\frac{1}{2}K_{\xi_3}\Delta\tau^{\mathrm{T}}\Delta\tau + K_{\xi_3}\xi^{\mathrm{T}}\Delta\tau \\ &\quad -2^{\frac{r_0+1}{2}}\lambda_{\min}\left(K_{\tilde{\zeta}_2}\right)V_{FCADS}^{\frac{r_0+1}{2}} \end{aligned} \tag{33}$$

The state vector $\xi = \left[\tilde{\xi}_1, \tilde{\xi}_2, \xi_3\right]^{\mathrm{T}}$ converges to 0 in finite time when $\lambda_{\min}\left(K_{\tilde{\zeta}_1}\right) > \frac{1}{2}K_{\tilde{\zeta}_3}$. Theorem 1 is proved

Then, the control law for dynamic positioning state feedback is developed as

$$\tau_{c0} = -K_3 S_3 + \tau + A_{tr}^{-1}\dot{\alpha}_2 + K_\xi \xi - S_2 \tag{34}$$

The formulation of the novel error vector is as follows.:

$$\hat{S}_1 = \hat{\eta} - \eta_d \tag{35}$$

$$\hat{S}_2 = \hat{v} - \hat{\alpha}_1 \tag{36}$$

$$\hat{S}_3 = \tau - \hat{\alpha}_2 \tag{37}$$

where

$$\hat{\alpha}_1 = -J^{\mathrm{T}}(\psi) K_1 \hat{S}_1 \tag{38}$$

$$\hat{\alpha}_2 = -K_2\hat{S}_2 - J^T(\psi)\hat{S}_1 + D\hat{v} - \hat{\tau}_d + M\dot{\hat{\alpha}}_1 \tag{39}$$

Noting the new error vector:

$$\tilde{S}_1 = \hat{S}_1 - S_1 \tag{40}$$

$$\tilde{S}_2 = \hat{S}_2 - S_2 \tag{41}$$

$$\tilde{S}_3 = \hat{S}_3 - S_3 \tag{42}$$

According to (11), (18), (24), and (45) yields

$$\begin{aligned} \tilde{S}_1^{\mathrm{T}}\tilde{S}_1 &= \left\|\hat{S}_1 - S_1\right\|^2 \\ &\leq \delta^2 B_1^2 \end{aligned} \tag{43}$$

According to (24), (40) and (51) yields

$$\begin{aligned} \|\hat{\alpha}_1 - \alpha_1\| &= \left\|-\mathrm{J}^{\mathrm{T}}(\psi)\mathrm{K}_1\hat{S}_1 + \mathrm{J}^{\mathrm{T}}(\psi)\mathrm{K}_1 S_1\right\| \\ &\leq \|\mathrm{K}_1\|\delta B_1 \end{aligned} \tag{44}$$

In the light of (11), (13), (4), (19), (24), (35), (44) and (46), we have

$$\begin{aligned} \tilde{S}_2^{\mathrm{T}}\tilde{S}_2 &= \left\|\hat{S}_2 - S_2\right\|^2 \\ &\leq (\|\hat{v} - v\| + \|K_1\| \|\hat{\eta} - \eta\|)^2 \\ &\leq \delta^2(B_2 + \|K_1\|B_1)^2 \end{aligned} \tag{45}$$

According to (10), (11), (18), (24), (35) and (40), we have

$$\begin{aligned} \left\|\dot{\hat{\alpha}}_1 - \dot{\alpha}_1\right\| &= \left\|\left(-\mathrm{J}^T(\psi)\mathrm{K}_1\hat{S}_1\right)' - (-\mathrm{J}^T(\psi)\mathrm{K}_1\mathrm{S}_1)'\right\| \\ &\leq \|\mathrm{S}^T(r)\|\|\mathrm{K}_1\|\delta\mathrm{B}_1 + \|\mathrm{K}_1\|\delta\mathrm{B}_2 \end{aligned} \tag{46}$$

where $S(r) = \begin{bmatrix} 0 & -r & 0 \\ r & 0 & 0 \\ 0 & 0 & 0 \end{bmatrix}$

Since η and $\dot{\eta}$ are bounded, according to (1) v is bounded, then r is bounded. Then $S(r)$ is bounded.

Set

$$\|\mathrm{S}(r)\| = \|\mathrm{S}^T(r)\| \leq \mathrm{B}_3 \tag{47}$$

where B_3 is a positive constant.

Hence, according (46) and (47)

$$\left\|\dot{\hat{\alpha}}_1 - \dot{\alpha}_1\right\| \leq \|K_1\|\delta(B_1 B_3 + B_2) \tag{48}$$

Similarly,

$$\left\|\dot{\hat{\alpha}}_2 - \dot{\alpha}_2\right\| \leq B_4 \tag{49}$$

where B_4 is a positive constant.

According to (43), (45), (13) and (48), we have

$$\|\widehat{\alpha}_2-\alpha_2\| \le \|K_2\|\delta(B_2+\|K_1\|B_1)+\delta B_1+\| D \| \delta B_2 + \sqrt[4]{2V_{do}(0)}+\| M \| \|K_1\|\delta(B_1B_3+B_2) \quad (50)$$

Then, according to (42), (37), (20) and (50), we have

$$\tilde{s}_3^T\tilde{s}_3 \le (\|K_2\|\delta(B_2+\|K_1\|B_1)+\delta B_1+\| D \| \delta B_2 + \sqrt[4]{2V_{do}(0)}+\| M \| \|K_1\|\delta(B_1B_3+B_2))^2 \quad (51)$$

Therefore, the control law for dynamic positioning using output feedback is formulated as:

$$\tau_c=-K_3\hat{S}_3+\tau+A_{tr}^{-1}\widehat{\alpha}_2+K_\zeta\hat{\xi}-\hat{S}_2 \quad (52)$$

IV. System Stability Analysis

Establish the Lyapunov function candidate as following:

$$V=\frac{1}{2}S_1^TS_1+\frac{1}{2}S_2^TMS_2+\frac{1}{2}S_3^TA_{tr}^{-1}S_3+\frac{1}{2}\xi^T\xi+\frac{1}{2}\tilde{p}^T\tilde{p} \quad (53)$$

Derivation of (53), we have

$$\dot{V}=S_1^T\dot{S}_1+S_2^TM\dot{S}_2+S_3^TA_{tr}^{-1}\dot{S}_3+\xi^T\dot{\xi}+\tilde{p}^T\dot{\hat{p}} \quad (54)$$

According to (19), (21), (24), Young's inequality and $\| J(\psi) \|=1$, we get

$$\begin{aligned} S_1^T\dot{S}_1 &= S_1^TJ(\psi)(S_2+\alpha_1) \\ &\le -S_1^TK_1S_1+\frac{1}{2}S_1^TS_1+\frac{1}{2}S_2^TS_2 \end{aligned} \quad (55)$$

According to (20), (26), (29), $\| J(\psi) \|=1$, $\tilde{\tau}_d=\tau_d-\hat{\tau}_d$,and Young's inequality and we get

$$\begin{aligned} S_2^TM\dot{S}_2 &= S_2^T(-Dv+\tau+\tau_d-M\dot{d}_1) \\ &\le -S_2^TK_2S_2-\frac{1}{2}S_1^TS_1+\frac{1}{2}S_2^TS_2+\frac{1}{2}S_3^TS_3+\frac{1}{2}\tilde{\tau}_d^T\tilde{\tau}_d \end{aligned} \quad (56)$$

When $\| \boldsymbol{\xi} \| \ge \xi_0$, according to (42) and Young's inequality, we get

$$\begin{aligned} \xi^T\dot{\xi} &= -\xi^TK_{\xi_1}\xi-\sum_{i=1}^{3}K_{\zeta_{2,i}}|\xi_i|^{r_0+1}-\sum_{i=1}^{3}\left|\hat{s}_{3,i}\,\Delta\tau_i\right| \\ &\quad -\frac{1}{2}K_{\zeta_3}\Delta\tau^T\Delta\tau+K_{\xi_3}\xi^T\Delta\tau \\ &\le -\xi^TK_{\xi_1}\xi-\textstyle\sum_{i=1}^{3}\left|\hat{s}_{3,i}\,\Delta\tau_i\right|+\frac{1}{2}K_{\xi_3}\xi^T\xi \end{aligned} \quad (57)$$

When $\| \boldsymbol{\xi} \| < \tilde{\xi}_0$ according to (31) and Young's inequality, we get

$$\xi^T\dot{\xi}=0 \quad (58)$$

$$\frac{1}{2}\xi^TK_\xi^TK_\xi\xi<-\frac{1}{2}\xi^TK_\xi^TK_\xi\xi+\xi_0^2\|K_\xi^TK_\xi\| \quad (59)$$

$$S_3^T\Delta\tau\le\frac{1}{2}S_3^TS_3+\frac{1}{2}\| \Delta\tau \|^2 \quad (60)$$

In (61), according to (42), (51) and Young's inequality yields

$$\begin{aligned} S_3^T\Delta\tau-\textstyle\sum_{i=1}^{3}\left|\hat{s}_{3,i}\,\Delta\tau_i\right| &= S_3^T\Delta\tau-\hat{S}_3^T\Delta\tau \\ &\le \frac{1}{2}(\|K_2\|\delta(B_2+\|K_1\|B_1)+\delta B_1 \\ &\quad +\| \mathbf{D} \| \delta B_2+\sqrt[4]{2V_{do}(0)} \end{aligned} \quad (61)$$

According to (57) (62), we get

$$\dot{V}\le-2\mu_1V+C_1 \quad (62)$$

where

$$C_1=\frac{1}{2}B_4^2+\frac{1}{2}\gamma^2-\frac{1}{2}\delta^2(B_2+\|K_1\|B_1)^2 +\frac{1}{2}\sqrt{2V_{do}(0)e^{-2D_{1\min}t}} \quad (63)$$

$$\mu_1=\min\left\{\lambda_{\min}(K_1),\lambda_{\min}\left[\left(K_2-\frac{1}{2}I_{3\times3}\right)M_0^{-1}\right],\right. \quad (64)$$

$$\lambda_{\min}\left[\left(K_3-\frac{1}{2}A_{tr}^{-1}(A_{tr}^{-1})^T+\frac{1}{2}K_3K_3^T\right)A_{tr}\right] \quad (65)$$

$$\left.\lambda_{\min}\left(K_{\xi_1}-\frac{1}{2}K_\xi^TK_\xi-\frac{1}{2}K_{\zeta_3}I_{3\times3}\right),\lambda_{\min}(D_1)\right\} \quad (66)$$

Satisfying

$$\lambda_{\min}(K_1)>0 \quad (67)$$

$$\lambda_{\min}(K_2)>\frac{1}{2} \quad (68)$$

$$\lambda_{\min}\left(K_3-\frac{1}{2}A_{tr}^{-1}(A_{tr}^{-1})^T+\frac{1}{2}K_3K_3^T\right)>0 \quad (69)$$

$$\lambda_{\min}\left(K_{\xi_1}-\frac{1}{2}K_\xi^TK_\xi-\frac{1}{2}K_{\tilde{\zeta}_3}I_{3\times3}\right)>0 \quad (70)$$

$$\lambda_{\min}(D_1)>0 \quad (71)$$

When $\| \boldsymbol{\xi} \| \ge \tilde{\xi}_0$, substituting (55)-(56), (58)-(60) into (54), we get

$$\dot{V}\le-2\mu_2\mathrm{V}+C_2 \quad (72)$$

where

$$\mu_2=\min\left\{\lambda_{\min}(\mathrm{K}_1),\lambda_{\min}\left[\left(\mathrm{K}_2-\frac{1}{2}\mathrm{I}_{3\times3}\right)\mathrm{M}_0^{-1}\right],\right. \quad (73)$$

$$\lambda_{\min}\left[\left(\mathrm{K}_3-\frac{1}{2}\mathrm{A}_{tr}^{-1}(\mathrm{A}_{tr}^{-1})^T+\frac{1}{2}\mathrm{K}_3\mathrm{K}_3^T-\frac{1}{2}\mathrm{I}_{3\times3}\right)\mathrm{A}_{tr}\right] \quad (74)$$

$$\left.\frac{1}{2}\lambda_{\min}(\mathrm{K}_\xi^T\mathrm{K}_\xi),\lambda_{\min}(\mathrm{D}_1)\right\} \quad (75)$$

Satisfying

$$\lambda_{\min}(\mathbf{K_1})>0 \quad (76)$$

$$\lambda_{\min}(\mathrm{K}_2)>\frac{1}{2} \quad (77)$$

$$\lambda_{\min}\left(\mathrm{K}_3-\frac{1}{2}\mathrm{A}_{\mathrm{tr}}^{-1}(\mathrm{A}_{\mathrm{tr}}^{-1})^T+\frac{1}{2}\mathrm{K}_3\mathrm{K}_3^T-\frac{1}{2}\mathrm{I}_{3\times3}\right)>0 \quad (78)$$

$$\lambda_{\min}(\mathrm{K}_\xi^T\mathrm{K}_\xi)>0 \quad (79)$$

$$\lambda_{\min}(\mathrm{D}_1)>0 \quad (80)$$

Substituting (64) and (74) yields

$$\dot{V}\le-2\mu V+C \quad (81)$$

where $\mu=\min\{\mu_1,\mu_2\}$ and $C=\max\{C_1,C_2\}$

V. Simulation and Comparison Studies

This section entails the execution of dynamic positioning simulation experiments aimed at elucidating the effectiveness of the suggested control strategy. Here, an example involving a supply vessel named Northern Clipper is provided., measuring 76.2 m in length and weighing 4.591 × 10^6 kg, is simulated utilizing the provided model parameters along with the thruster specifications detailed as follows:

$$M=\begin{bmatrix} 5.3122\times10^6 & 0 & 0 \\ 0 & 8.2831\times10^6 & 0 \\ 0 & 0 & 3.7454\times10^9 \end{bmatrix} \quad (82)$$

$$\mathrm{D}=\begin{bmatrix} 5.0242\times10^4 & 0 & 0 \\ 0 & 2.7229\times10^5 & -4.3933\times10^6 \\ 0 & -4.3933\times10^6 & 4.1894\times10^8 \end{bmatrix} \quad (83)$$

$$A_{tr}=\begin{bmatrix} 0.2 & 0 & 0 \\ 0 & 0.2 & 0 \\ 0 & 0 & 0.2 \end{bmatrix} \quad (84)$$

The investigation addresses the input saturation of the ship's thrusters, and Table 1 delineates the restrictions concerning the input saturation of the supply vessel's thrusters.

The scene parameters are set as $\mathrm{b}(0) = [10kN, 10kN, 10kN]^T$, $\mathrm{T} = \mathrm{diag}(10^3, 10^3, 10^3)$, $\Psi = \mathrm{diag}(3\times10^4, 3\times10^3, 3\times10^5)$.

TABLE I. THRUSTER INPUT SATURATION LIMIT VALUES IN SURGE, SWAY, AND YAW

	Thrusters	Limit values
In surge	τ_{M1}	3.76815 * 10^2(KN)
In sway	τ_{M2}	6.8072 * 10^2(KN)
In yaw	τ_{M3}	7.31 * 10^2(KN)

The targeted ship location and orientation are $\eta_d = [0m, 0m, 0°]^T$ and the initial states are $\eta(0) = [20\text{ m}, 20\text{ m}, 10°]^T$, $v(0) = [0\text{ m/s}, 0\text{ m/s}, 0°/s]^T$, $\tau(0) = [0,0,0]^T$, $\xi(0) = [5\times10^4, 5\times10^4, 5\times10^4]^T$, $\hat{\eta}(0) = [20\text{ m}, 20\text{ m}, 10°]^T$, $\hat{\zeta}(0) = [2,2,0.4]^T$, $\hat{\sigma}(0) = [0,0,0]^T$, The design parameters are $\alpha_1 = 25, \alpha_3 = 20$, $\mathrm{K}_1 = \mathrm{diag}(0.1,0.1,0.1)$, $\mathrm{K}_2 = \mathrm{diag}(1\times10^7, 1\times10^7, 8\times10^9)$, $\mathrm{K}_{\xi1} = \mathrm{diag}(5,3,5)$, $\mathrm{K}_{\xi2} = \mathrm{diag}(2,2,5)$, $K_{\xi3} = 0.02$, $\xi_0 = 20$, $r_0 = \frac{6}{7}$, $\mathrm{K}_3 = \mathrm{diag}(0.8,0.8,0.8)$ and $\mathrm{K}_\xi = \mathrm{diag}(5,5,5)$.

The contrast between the control law presented herein, incorporating thruster system dynamics, and the control strategy addressed in [7]., which disregards these dynamics, highlights the smoother transitions and improved alignment with engineering principles exhibited by the control law proposed in this paper.

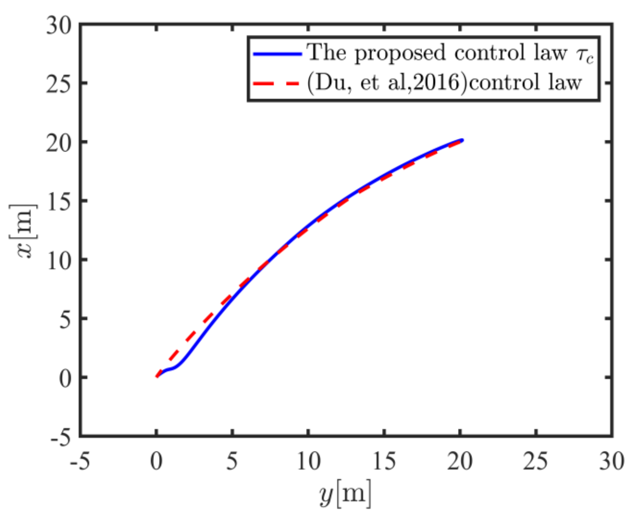

Fig. 1. Horizontal motion trajectory of the ship.

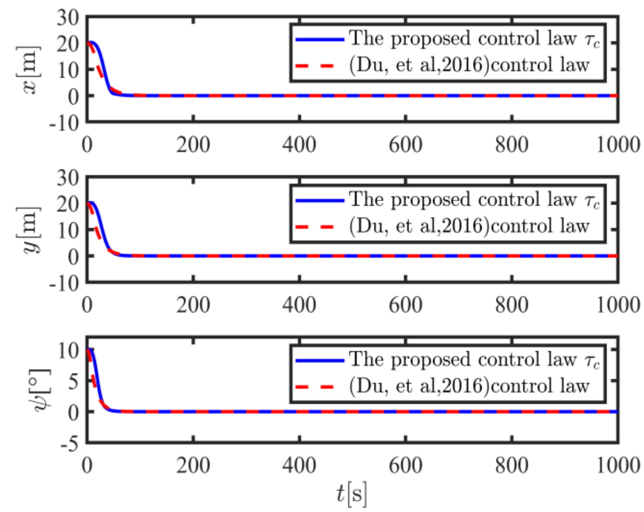

Fig. 2. Ship position and heading.

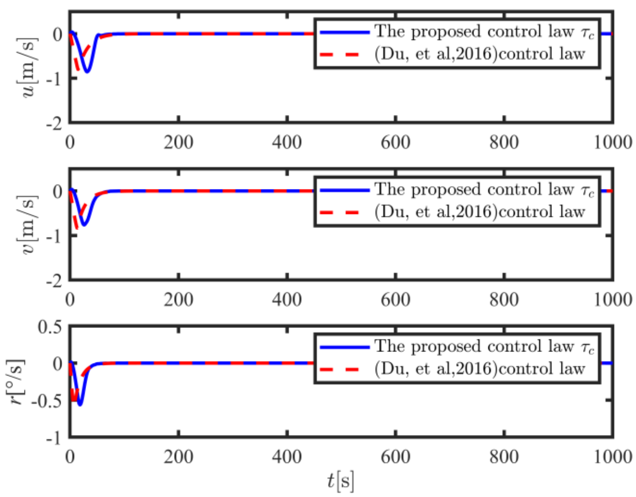

Fig. 3. Ship speed.

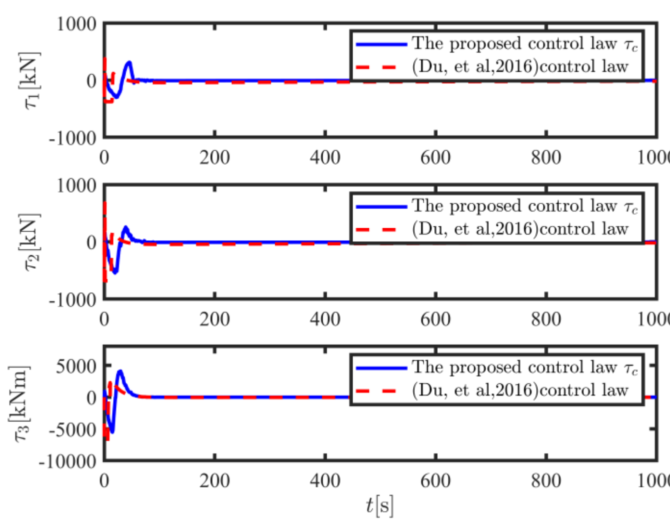

Fig. 4. Actual thrust of the ship

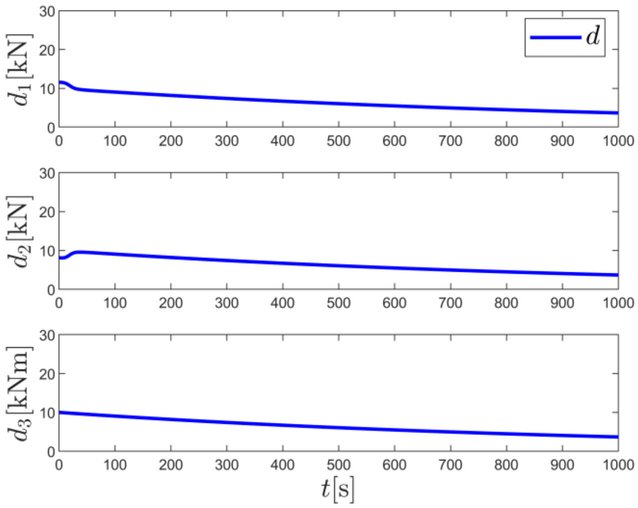

Fig. 5. External interference forces on ships

The continuous lines in Figs. 1-4 depict the simulation results of the dynamic positioning control algorithm τ_c proposed in this study, while the dotted lines illustrate the simulation outcomes of control law τ_0 suggested in [7]

In Fig.4, The control methodology advocated in this paper generates a smooth control variable without any sudden changes. In contrast, the control method described in [7] exhibits significant fluctuations and abrupt variations in the control signal, particularly around the initial time period. This underscores the practicality and relevance of the control law proposed in this paper compared to the approach described in [7], as it more closely aligns with engineering reality. Fig.5 shows the external interference forces on the ship.

VI. Conclusion

This paper proposes a new backstepping controller that considers the dynamic characteristics of ship propulsion systems when a ship is subjected to unknown time-varying disturbances, in response to the problem of unmeasurable and input saturation of the ship. The controller combines a high gain State observer, a finite time Auxiliary power unit and a backstepping controller, which is obviously different from the traditional backstepping controller. Finally, this paper considers the dynamic characteristics of the propulsion system to ensure that the control signal generated by the controller remains stable and does not undergo sudden changes, regardless of whether the ship is under strong or weak interference.

Future research will concentrate on two primary areas. Firstly, the refinement of the control algorithm proposed in this paper will be pursued to adeptly address dynamic positioning control complexities under diverse marine conditions. Secondly, investigations will extend to dynamic positioning scenarios encompassing varying initial yaw angles, with a further extension of the study into automated berthing applications.

References

[1] Yang Y, Du J, Liu H, et al. A trajectory tracking robust controller of surface vessels with disturbance uncertainties[J]. IEEE Transactions on Control Systems Technology, 2014, 22(4): 1511-1518.

[2] I., T., 2012. Fossen Handbook of Marine Craft Hydrodynamics and Motion Control. John Wiley, Norway.

[3] Hu X, Du J, Zhu G, et al. Robust adaptive NN control of dynamically positioned vessels under input constraints[J]. Neurocomputing, 2018, 318: 201 212.

[4] D. Mu, Y. Feng and G. Wang, Y. Fan, and Y. Zhao, "Single-parameter-learning-based robust adaptive control of dynamic positioning ships considering thruster system dynamics in the input saturation state," NonlinearDynamics, vol. 110, pp. 395-412, 2022

[5] D. Mu, Y. Feng and G. Wang, "State-unknown single parameter learning adaptive output feedback control for ship dynamic positioning," Ocean Engineering, vol. 266, p. 112811, 2022.

[6] D. Mu, Y. Feng, G. Wang, Y. Fan, Y. Zhao, and X. Sun, "Ship Dynamic Positioning Output Feedback Control with Position Constraint Considering Thruster System Dynamics," Journal of Marine Science and Engineering, vol. 11, p. 94, 2023-01-04 2023

[7] Du J, Hu X, Krstic M, et al. Robust dynamic positioning of ships with disturbances under input saturation[J]. Automatica, 2016, 73: 207 214.